

Mechanisms of trichostatin A inhibiting AGS proliferation and identification of lysine-acetylated proteins

Yu-Gang Wang, Na Wang, Guang-Ming Li, Wen-Li Fang, Jue Wei, Jia-Li Ma, Ting Wang, Min Shi

Yu-Gang Wang, Na Wang, Wen-Li Fang, Jue Wei, Jia-Li Ma, Ting Wang, Min Shi, Department of Gastroenterology, Shanghai Changning Central Hospital, Shanghai 200336, China
Guang-Ming Li, Department of Gastroenterology, Xinhua Hospital, Shanghai Second Medical University, Shanghai 200092, China

Author contributions: Wang YG, Wang N and Shi M designed the study; Wang YG, Wang N, Li GM, Fang WL, Wei J, Wang T and Shi M carried out the study; Wang YG, Wang N, Li GM, Fang WL, Wei J, Wang T and Shi M contributed new reagents and analytic tools; Wang YG, Wei J and Ma JL analyzed the data; Wang YG, Wang N and Shi M wrote the paper.

Supported by Shanghai Municipal Health Bureau Key Disciplines Grant, No. ZK2012A05; National Natural Science Foundation, No. 81070344

Correspondence to: Min Shi, MD, PhD, Department of Gastroenterology, Shanghai Changning Central Hospital, No. 1111 Xianxia Road, Changning district, Shanghai 200336, China. shimingdyx@yeah.net

Telephone: +86-21-62909911 Fax: +86-21-62906478

Received: January 16, 2013 Revised: March 21, 2013

Accepted: April 9, 2013

Published online: June 7, 2013

Abstract

AIM: To explore the effect of lysine acetylation in related proteins on regulation of the proliferation of gastric cancer cells, and determine the lysine-acetylated proteins and the acetylated modified sites in AGS gastric cancer cells.

METHODS: The CCK-8 experiment and flow cytometry were used to observe the changes in proliferation and cycle of AGS cells treated with trichostatin A (TSA). Real time polymerase chain reaction and Western blotting were used to observe expression changes in p21, p53, Bax, Bcl-2, CDK2, and CyclinD1 in gastric cancer cells exposed to TSA. Cytoplasmic proteins in gastric cancer cells before and after TSA treatment were immunoprecipitated with anti-acetylated lysine antibodies, separated using sodium dodecyl sulfate polyacrylamide

gel electrophoresis gel and silver-stained to detect the proteins by mass spectrometry after removal of the gel. The acetylated proteins in AGS cells were enriched with lysine-acetylated antibodies, and a high-resolution mass spectrometer was used to detect the acetylated proteins and modified sites.

RESULTS: TSA significantly inhibited AGS cell proliferation, and promoted cell apoptosis, leading to AGS cell cycle arrest in G0/G1 and G2/M phases, especially G0/G1 phase. p21, p53 and Bax gene expression levels in AGS cells were increased with TSA treatment duration; Bcl-2, CDK2, and CyclinD1 gene expression levels were decreased with TSA treatment duration. Two unknown protein bands, 72 kDa (before exposure to TSA) and 28 kDa (after exposure to TSA), were identified by silver-staining after immunoprecipitation of AGS cells with the lysine-acetylated monoclonal antibodies. Mass spectrometry showed that the 72 kDa protein band may be PKM2 and the 28 kDa protein band may be ATP5O. The acetylated proteins and modified sites in AGS cells were determined.

CONCLUSION: TSA can inhibit gastric cancer cell proliferation, which possibly activated signaling pathways in a variety of tumor-associated factors. ATP5O was obviously acetylated in AGS cells following TSA treatment.

© 2013 Baishideng. All rights reserved.

Key words: Trichostatin A; Acetylation modification; Gastric cancer; Mass spectrometry; ATP5O; PKM2

Core tip: Previous research has shown that deacetyltransferase inhibitors not only induce cell cycle arrest, differentiation and apoptosis of many tumor cells *in vitro*, but also inhibit tumor growth in tumor-bearing animals. They are through the acetylation modification of deacetyltransferase inhibitor on histone. Only a few studies have focused on the acetylation modification by deacetyltransferase on non-histone. This is the first study to identify acetylated proteins in gastric cancer

cells before and after exposure to trichostatin A to explore the effect of lysine acetylation of related proteins on the regulation of gastric cancer cell proliferation. Moreover, the lysine-acetylated proteins and the modified sites in AGS cells were assessed. We explored whether ATP5O was obviously acetylated after trichostatin A treatment in AGS cells.

Wang YG, Wang N, Li GM, Fang WL, Wei J, Ma JL, Wang T, Shi M. Mechanisms of trichostatin A inhibiting AGS proliferation and identification of lysine-acetylated proteins. *World J Gastroenterol* 2013; 19(21): 3226-3240 Available from: URL: <http://www.wjgnet.com/1007-9327/full/v19/i21/3226.htm> DOI: <http://dx.doi.org/10.3748/wjg.v19.i21.3226>

INTRODUCTION

Gastric cancer has a high incidence and mortality worldwide, especially in East Asia^[1,2]. More than 400000 new patients with gastric cancer are diagnosed in China every year. The prevalence and mortality of this disease in China are higher than the world average values^[3]. In the absence of targets, traditional chemotherapy has severe side effects. Therefore, cancer treatment and research are now focusing on molecular targeted therapy due to its high selectivity, good efficacy and reduced side effects.

Histone acetylation/deacetylation modification, one of the essential mechanisms of gene transcriptional regulation, occurs mainly in conservative lysine residues on histone H3 and H4 tails, which are regulated by histone acetyltransferases and histone deacetylases (HDACs). Significantly increased activity of HDACs leads to an expression imbalance of some molecules affecting cell proliferation, apoptosis and cell cycle, thus causing cancer^[4]. A large number of studies have shown that deacetyltransferase inhibitors not only induce cell cycle arrest, differentiation and apoptosis of many tumor cells *in vitro*, but also inhibit tumor growth in tumor-bearing animals^[5,6]. There have been numerous studies on the acetylation modification by deacetyltransferase inhibitors on histone, however, studies focusing on the acetylation modification by deacetyltransferase on non-histones are rare. Further studies are needed to investigate the acetylated non-histones involved in tumor growth and metabolism, and the signaling pathways through which these proteins induce tumor apoptosis. We treated AGS gastric cancer cells with the histone deacetyltransferase inhibitor, trichostatin A (TSA), to identify differentially acetylated non-histones before and after TSA treatment. We also explored the apoptosis and proliferation mechanisms of gastric cancer cells.

MATERIALS AND METHODS

Materials

AGS cells were purchased from the Cell Resource Center of Shanghai Institutes for Biological Sciences, Chinese Academy of Sciences; Ham's F12 medium was from

HyClone; trypsin-EDTA solution and fetal bovine serum from Invitrogen; the cell counting kit-8 (CCK-8) from Dojindo Company; TSA from Sigma (batch number T1952); the Annexin V-FITC Apoptosis Detection Kit, FACS Calibur and LSR™ II Flow Cytometer from BD Pharmingen; the primer was designed by Shanghai Sangon Biotech Co., Ltd.; Agarose I™ was from Amresco, the RNeasy Mini Kit from Qiagen; the Reverse Transcription System from Promega; SYBR® Premix Ex Taq™ from TaKaRa; ABI prism 7300 polymerase chain reaction (PCR) from ABI; Amersham ECL plus the Western blotting Detection System and CNBr Activated Sepharose 4B from GE; Pierce BCA Protein Assay Kit from Thermo; Acetyl- α -Tubulin (Lys40) (D20G3) XP® Rabbit mAb from CST; Goat anti-rabbit IgG-HRP from Sigma; LTQ VELOS from Thermo Finnigan, and anti-ATP5O and anti-PKM2 antibodies from Sigma.

CCK-8 experiment

AGS cell strains were cultured in Ham's F12 medium + 10% FBS for 24 h and divided into 8 groups (3 holes in each group). The media in the holes were added to complete media containing TSA at final concentrations of 0, 0.015, 0.03, 0.06, 0.1, 0.25, 0.5 and 1 $\mu\text{mol/L}$, respectively. The complete media were incubated with 5% CO₂ at 37 °C for 72 h, and then added to CCK-8 solution in the proportion of 100 μL /10 μL , and left to stand at 37 °C for 1 h. Absorbance was then read at a wavelength of 450 nm using a microplate reader.

Detection of cell apoptosis and cycle by flow cytometry

Two dishes of AGS cells cultured for 24 h were added to complete medium containing TSA at a final concentration of 0.25 $\mu\text{mol/L}$, and a further two dishes of cultured cells were added to new medium as a control. The media were incubated with 5% CO₂ at 37 °C for 24 h, centrifuged, transferred to a 5 mL culture tube and the supernatant was removed. The cells were re-suspended, and 5 μL Annexin V-FITC and propidium iodide (PI) were added, incubated in the dark at 20-25 °C for 15 min and then 400 μL Annexin V binding solution was added for flow cytometry. Annexin V-FITC had green fluorescence and PI had red fluorescence. The wavelength of light excited by flow cytometry was adjusted to 488 nm. FITC fluorescence was detected with a band-pass filter of 515 nm and PI fluorescence was detected with a filter of more than 560 nm. In addition, the cell sediments were added to 1 mL of 70% ethanol, fixed, washed, centrifuged twice, re-suspended in 0.5 mL PBS containing 50 $\mu\text{g/mL}$ PI and 100 $\mu\text{g/mL}$ RNase A, and incubated in the dark at 37 °C for 30 min to determine the cell cycle using a flow cytometer according to standard procedures. The results were analyzed using a cycle meter and the software FlowJo6.3^[7].

Real-time polymerase chain reaction

AGS cells cultured for 24 h were added to complete medium containing TSA at final concentrations of 0 and 0.25 $\mu\text{mol/L}$, respectively (the former for the control).

Table 1 Oligonucleotide sequences used in real-time polymerase chain reaction

Gene	Primer (5' to 3')	Length (bp)
<i>β-actin</i>	F: 5'TGGAGAAAATCTGGCACCA3' R: 5'CAGGCGTACAGGGATAGCAC3'	189
<i>p21</i>	F: 5'TCCAAGAGGAAGCCCTAATCC3' R: 5'ACAACTGAGACTAAGGCAGAAGATG3'	101
<i>p53</i>	F: 5'TCAGTCTACCTCCCGCCATAA3' R: 5'GTGCAGGCCAACTTGTTCAGT3'	231
<i>Bcl-2</i>	F: 5'CTTTTCTACTTTGCCAGCAAAAC3' R: 5'GAGGCCGTCCCAACCAC3'	149
<i>CDK2</i>	F: 5'GCTAGCAGACTTTGGACTAGCCAG3' R: 5'AGCTCGGTACCACAGGGTCA3'	85
<i>CyclinD1</i>	F: 5'AACAGAAGTGCGAGGAGGAG3' R: 5'CTGGCATTTTGGAGAGGAAG3'	299
<i>Bax</i>	F: 5'CCAGGGTGGTTGGGTGAGACT3' R: 5'TGGGAGGTCAGCAGGGTAGAT3'	231

Bcl-2: B cell lymphoma-2; CDK2: Cyclin-dependent kinase 2; Bax: Bcl-associated X protein.

The total RNA in all samples was extracted, quantified and reversely transcribed according to the Qiagen kit instructions. Fluorescence quantitative PCR was carried out on p21, p53, Bax, Bcl-2, CDK2 and CyclinD1, followed by data collection and analysis. The PCR primer sequences and fragment lengths are shown in Table 1.

Western blotting

One dish of AGS cells cultured for 24 h was used as the 0 h sample, and a further 2 dishes of cells were added to medium containing a final concentration of 0.25 μmol/L TSA, and incubated with 5% CO₂ at 37 °C for 12 and 24 h, respectively. The cells were collected after digestion with pancreatin, washed twice with PBS, centrifuged to remove the supernatant, collected and placed on ice for lysis. The proteins were quantified using the BCA method. Protein electrophoresis sodium dodecyl sulfate polyacrylamide gel electrophoresis, membrane-transfer, immunoreactions, development and gel electrophoresis image analysis were performed for p21, p53, Bax, Bcl-2, CDK and CyclinD1.

Enrichment of lysine-acetylated proteins

Five dishes of AGS cells were added to complete medium containing a final concentration of 0.5 μmol/L TSA, and another five dishes of cells were directly placed in new medium as the control. Cell lysis was performed after incubation in the medium for 24 h, and all protein concentrations were adjusted to 5 mg/mL after determination using the BCA method. Total protein of 20 mg and lysine-acetylated mAb of 0.5 mL (CNBr Activated Sepharose 4B) were mixed, incubated in a table concentrator at 4 °C for 5 h, washed 3 times and collected for vacuum drying. The lysine-acetylated proteins were enriched and dissolved in PBS. Electrophoresis, silver-staining and photographs of the total proteins of 2 μg taken from each dish after the proteins were quantified with BCA were carried out. Western blotting was performed

on all proteins in each group to determine the effect of acetylation (20 μg total protein from AGS cells not treated and treated with 0.5 μmol/L TSA, respectively; 20 μg flow-through proteins incubated with the antibody gel column in AGS cells not treated and treated with 0.5 μmol/L TSA respectively; and 100 ng total proteins enriched after incubation with antibody gel column in AGS not treated and treated with 0.5 μmol/L TSA, respectively). Acetyl-α-tubulin (Lys40) (D20G3) XP® Rabbit mAb was the primary antibody and Goat anti-rabbit IgG-HRP was the secondary antibody.

Identification of in-gel protein with mass spectrometry

The enriched protein band on silver-stained gel (72 kDa before exposure to TSA and 28 kDa after exposure to TSA), was broken down in the gel with enzyme (trypsin for 20 h), and the decomposed peptide was extracted for ESI MS detection. After the chromatographic column was equilibrated with 95% solution A (0.1% formic acid solution), the sample was fed into a Trap column. From 0 to 50 min, the linear gradient of solution B (78% acetonitrile solution containing 0.1% formic acid) increased from 4% to 50%; from 50 to 54 min, the linear gradient of solution B increased from 50% to 100%; from 54 to 60 min, the linear gradient of solution B was maintained at 100%. Twenty fragmentographies (MS2 scan) were collected by mass-to-charge ratio of the polypeptides and polypeptide fragments after full scan. The raw file was searched with BOWWORKS software in the relevant database to determine the protein. The database was ipi. HUMAN.v3.53. SEQUEST screening parameters were as follows: when Charge + 1, Xcorr ≥ 1.9; when Charge + 2, Xcorr ≥ 2.2; and when Charge + 3, Xcorr ≥ 3.75; wherein DelCN ≥ 0.1.

Identification of acetylated sites using mass spectrometry

Experimental methods for cell lysis, protein extraction and acetylated peptides affinity enrichment were obtained from published techniques^[8]. The resulting peptides were assayed by continuous separation using SCX followed by C18 columns (Dionex, Sunnyvale, CA, United States) before being subjected to MS/MS analysis using an LTQ-Orbitrap mass spectrometer (Thermo Electron, Bremen, Germany).

Protein sequence database search and manual verification

The mass spectrometry data were initially searched against the NCBI database with the aid of the Sequest search engine. Searches for acetylated peptides were done against the *Homo sapiens* proteins database. The search engine MASCOT (Matrix Science, London, United Kingdom) was used for the database search, and extract_msn.exe version 4.0 was used for peaklist generation. A low cutoff of the peptide score of 20 was selected to maximize the identification of lysine-acetylated peptides. Trypsin was specified as the proteolytic enzyme, and up to 6 missed cleavage sites per peptide were allowed. Carbamidomethylation of cysteine was set as a fixed modification and

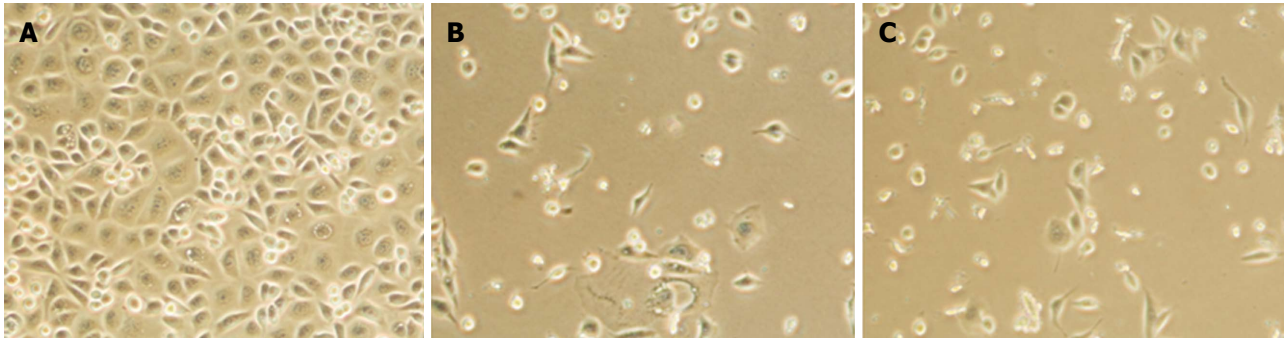


Figure 1 Proliferation of AGS cells exposed to different concentrations of trichostatin A for 72 h. A: AGS cells after treatment with 0 $\mu\text{mol/L}$ trichostatin A (TSA); B and C: AGS cells were significantly reduced after exposed to 0.25 $\mu\text{mol/L}$ TSA (B) and further reduced after treated with 0.5 $\mu\text{mol/L}$ TSA (C).

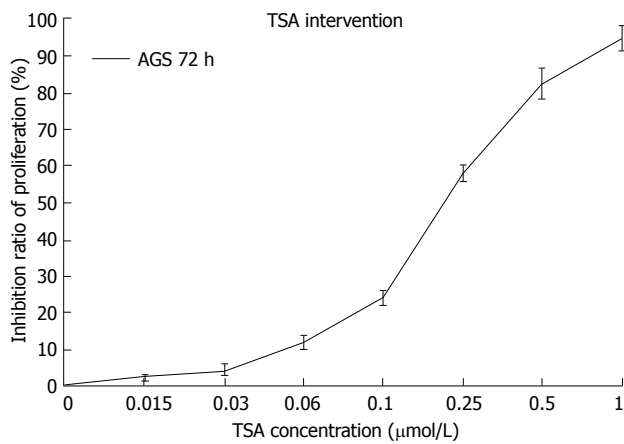


Figure 2 Effect of different concentrations of trichostatin A on inhibition of AGS cell proliferation in the cell counting kit-8 experiment. The inhibition of AGS cells was gradually increased with increasing trichostatin A concentration 0, 0.015, 0.03, 0.06, 0.1, 0.25, 0.5 and 1 $\mu\text{mol/L}$. TSA: Trichostatin A.

oxidation of methionine and acetylation of lysine as variable modifications. Charge states of +1, +2 or +3 were considered for parent ions. Mass tolerance was set to ± 4.0 Da for parent ion masses and ± 0.6 Da for fragment ion masses. Acetylated lysine-containing peptides identified with a MASCOT score of 25 were manually verified by the method described by Chen *et al*^[9].

Detection of acetylated proteins

One dish of normal AGS cells was collected as the 0 h sample after digestion with pancreatin, and a further 3 dishes of cells were added with a final concentration of 0.5 $\mu\text{mol/L}$ TSA and incubated with 5% CO_2 in an incubator at 37 $^{\circ}\text{C}$ for 6, 12 and 24 h. The collected cells were digested with pancreatin, re-suspended, and decomposed by ultrasound on ice. The decomposed cells were centrifuged at 15000 g and 4 $^{\circ}\text{C}$ for 30 min and the supernatant was obtained for identification of protein concentration using the BCA. Five mg of total protein was mixed with 50 μg of the M2 isoform of pyruvate kinase antibody (anti-PKM2) and the ATP synthase subunit O antibody (anti-ATP5O) (covalently cross-linked with CNBr Activated Sepharose 4B) and incubated in an incubator at 4 $^{\circ}\text{C}$ for 5 h. The gel column was washed 3 times and the

washed proteins were collected. The protein content of ATP5O^[10] and PKM2^[11] in the 4 samples was determined using Western blotting. After binding, the washed proteins with the anti-acetylated lysine antibodies, and the protein content of ATP5O and PKM2 in the 4 samples were detected using Western blotting.

RESULTS

Effect of TSA on AGS cell proliferation, apoptosis and cell cycle

CCK-8 experiments showed that AGS cells were significantly reduced after the addition of 0.25 $\mu\text{mol/L}$ TSA and AGS cell proliferation was more obviously inhibited after the addition of 0.5 $\mu\text{mol/L}$ TSA. Therefore, TSA significantly inhibited proliferation of the gastric cancer cell line (Figures 1 and 2). The bivariate scatter diagram of flow cytometry showed more apoptotic and necrotic AGS cells after treatment with 0.25 $\mu\text{mol/L}$ TSA (Figure 3). The flow cytometry cycle diagrams showed that the AGS cell cycle ratio before TSA treatment was as follows: %G1 = 26, %S = 53.5, %G2 = 17.7, and the AGS cell cycle ratio after 0.25 $\mu\text{mol/L}$ TSA treatment was as follows: %G1 = 44.6, %S = 20.9, %G2 = 31.3. Therefore, TSA induced apoptosis and necrosis of AGS cells, and cycle arrest mainly occurred in G0/G1 and G2/M phases, especially in G0/G1 phase (Figure 4).

Observation of p21, p53, Bax, Bcl-2, CDK2 and CyclinD1 expression levels after TSA treatment using real-time PCR and Western blotting

Real-time PCR results showed that more p21, p53 and Bax mRNA was expressed after AGS cells were exposed to 0.25 $\mu\text{mol/L}$ TSA, and the expression levels were increased with TSA treatment duration, while less Bcl-2, CDK2 and CyclinD1 mRNA was expressed after TSA treatment, and the expression levels were decreased with TSA treatment duration (Figure 5). The expression levels of the above six cell cycle-related proteins in AGS cells shown in Western blotting were the same as the levels shown in real-time PCR (Figure 6).

Enrichment of lysine-acetylated proteins

In AGS cells enriched with lysine-acetylated monoclonal

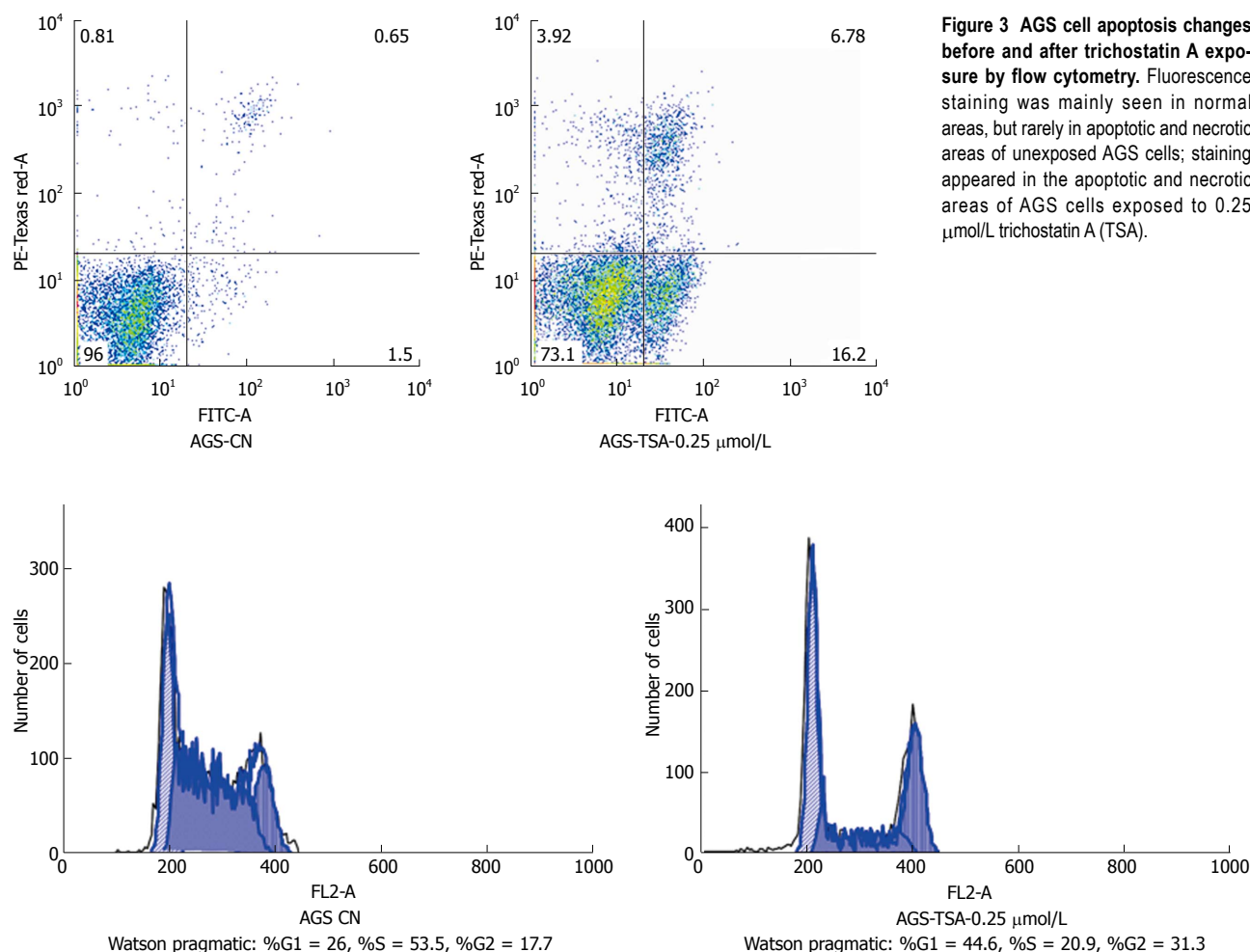


Figure 4 AGS cell cycle changes before and after trichostatin A exposure by flow cytometry. The AGS cell cycle ratio before TSA treatment was: %G1 = 26, %S = 53.5, %G2 = 17.7, and the AGS cell cycle ratio after 0.25 $\mu\text{mol/L}$ trichostatin A treatment was: %G1 = 44.6, %S = 20.9, %G2 = 31.3. Cycle arrest occurred in G0/G1, G2/M phases, especially in G0/G1 phase. TSA: Trichostatin A.

antibodies, the enriched proteins were located at 72 kDa before exposure to 0.5 $\mu\text{mol/L}$ TSA shown by silver-staining, but appeared at 55, 28 and 17 kDa after exposure to 0.5 $\mu\text{mol/L}$ TSA, which was consistent with the Western blotting results (Figure 7). Some studies have shown that the enriched proteins at 55 and 17 kDa were tubulin and histone protein, respectively. In our experiments which were designed to determine the modified proteins enriched by lysine-acetylated monoclonal antibodies, total protein in the cytoplasm, flow-through proteins, and enriched proteins all showed obvious bands. No obvious bands for these three proteins were found before TSA treatment (Figure 8), which indicated that the protein enrichment method with lysine-acetylated monoclonal antibodies was effective and credible.

Identification of in-gel proteins by mass spectrometry

Mass spectrometry was carried out on the unknown protein bands, 72 kDa (before TSA treatment) and 28 kDa (after TSA treatment), which were enriched and modified by lysine acetylation to obtain ESI MS total ion chromatography (Figure 9). We searched the protein database ipi.

HUMAN.v3.53 with the SEQUEST program according to the set screening parameters. The results indicated that 72 kDa (before TSA treatment) was PKM2, and 28 kDa (after TSA treatment) was ATP5O in AGS cells (Figure 10).

Identification of acetylated sites using mass spectrometry and detection of acetylated proteins

We screened all peptide sequences obtained by detection of the acetylated sites using mass spectrometry. In the plasmosin of normal AGS cells, we found 602 acetylated peptides, 171 unique peptides and 136 acetylated sites (Table 2). Cell cycle G0 analysis showed that the identified proteins contained chromatin, nucleosome, DNA components as well as chromatin modification, protein acetylation, glucose metabolism and other biological processes. These components were mainly involved in cellular components such as chromatin, nucleoplasm and organelles, and these molecular functions were mainly associated with cell proliferation and apoptosis (Figure 11). In these acetylated peptides, the presence of ATP5O indicated that ATP5O had modified sites (Figure 12). In the mass spectrometry results, most of the identified proteins had a

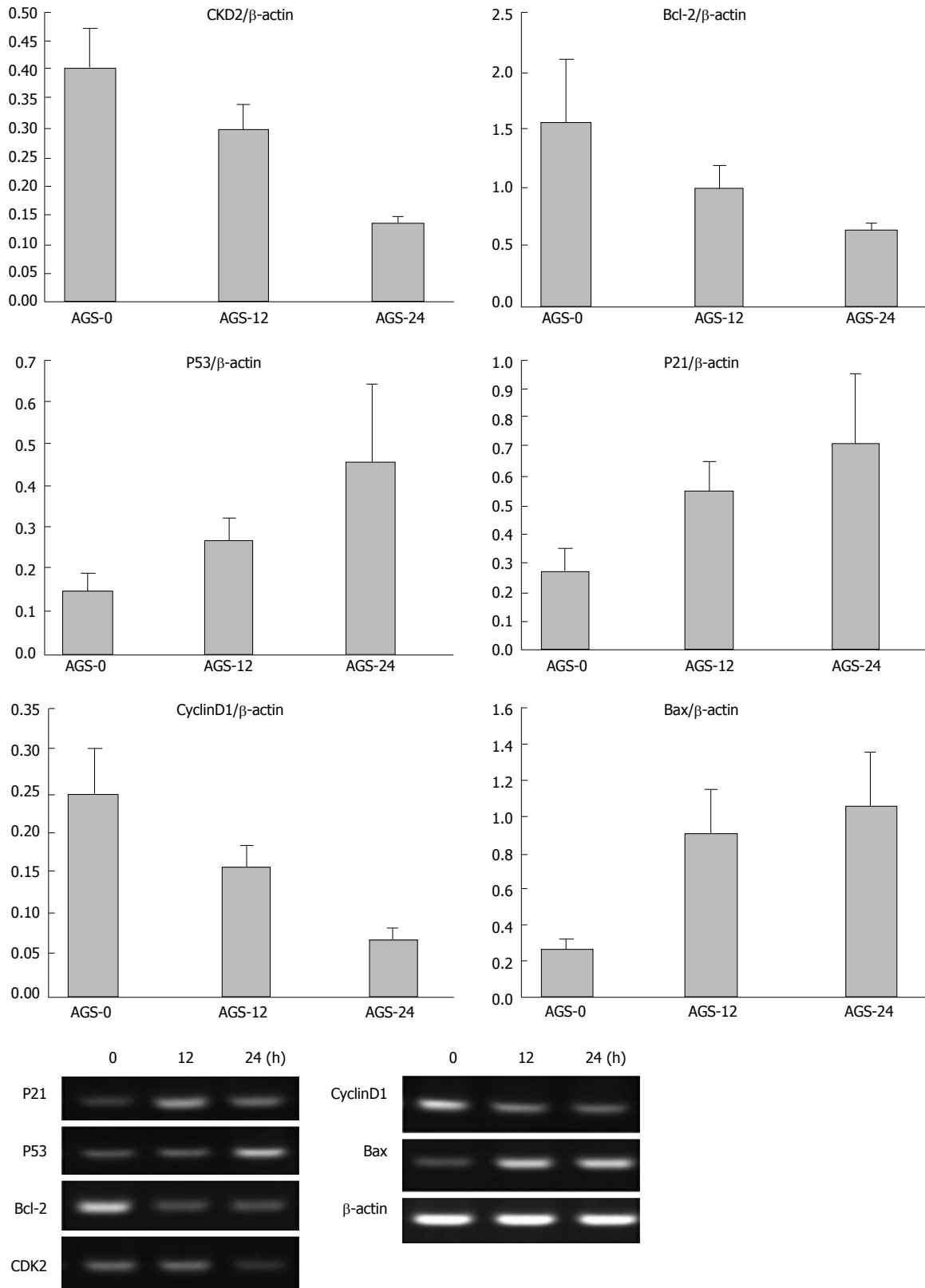


Figure 5 mRNA expression levels of p21, p53, Bax, Bcl-2, CDK2 and CyclinD1 in AGS cells exposed to 0.25 μ mol/L trichostatin A shown by real-time polymerase chain reaction. The mRNA expression levels of Bcl-2, CDK2 and CyclinD1 were decreased and the mRNA expression levels of p21, p53 and Bax were increased 12 h after AGS cells were exposed to 0.25 μ mol/L trichostatin A. The mRNA expression levels of Bcl-2, CDK2 and CyclinD1 were further decreased and the mRNA expression levels of p21, p53 and Bax were further increased 24 h after exposure.

cover percent greater than 20%, and a score greater than 25, which proved that the mass spectrometry identifica-

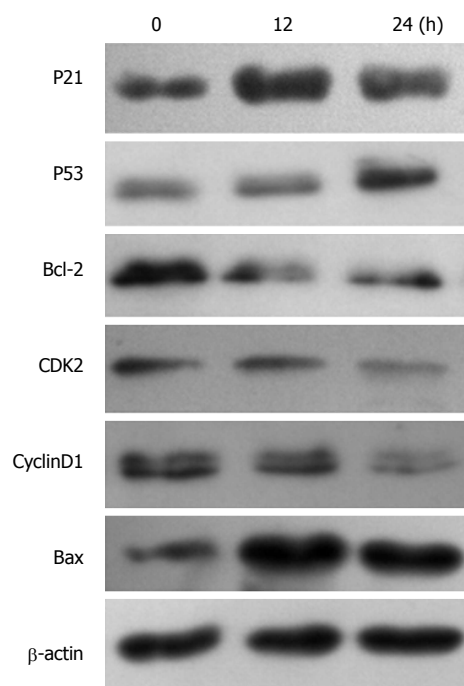


Figure 6 Protein expression levels of p21, p53, Bax, Bcl-2, CDK and cyclin after AGS cells were exposed to 0.25 $\mu\text{mol/L}$ trichostatin A shown by Western blotting. The protein expression levels of Bcl-2, CDK2 and CyclinD1 were decreased and the protein expression levels of p21, p53 and Bax were increased 12 h after AGS cells were exposed to 0.25 $\mu\text{mol/L}$ trichostatin A. The protein expression levels of Bcl-2, CDK2 and CyclinD1 were further decreased and the protein expression levels of p21, p53 and Bax were further increased 24 h after exposure.

tion results were correct. Further validation of the acetylated proteins, ATP5O and PKM2, showed that the total amount of ATP5O and PKM2 proteins did not change with the treatment duration of 0.5 $\mu\text{mol/L}$ TSA, however, more ATP5O was acetylated than PKM2 (Figure 13), which indicated acetylation of ATP5O and deacetylation of PKM2 after TSA treatment.

DISCUSSION

Modern oncology theories have revealed that genetic defects and gene epigenetic changes lead to malignant tumors. Epigenetics has shown acetylation of DNA methylation and histone, which are involved in gene transcription and expression, thus regulating DNA functions^[12-14]. TSA derives from a natural hydroxamic acid, HDACi, which inhibits the activity of HDACs by binding the hydroxamic acid ligand with zinc ions at the bottom of the HDAC tubular structure^[15]. Cancer research has discovered that TSA can arrest cell cycle, induce cell apoptosis, regulate cell differentiation and inhibit cell migration in the absence of cytotoxicity^[16-18]. We found that the proliferation of normally grown AGS gastric cancer cells was significantly inhibited after exposure to 0.25 $\mu\text{mol/L}$ TSA, *i.e.*, more apoptotic and necrotic cells. In addition, flow cytometry showed that the cycle arrest of AGS cells exposed to TSA occurred in G0/G1 and G2/M phases, which is consistent with other previous reports^[19-22]. In

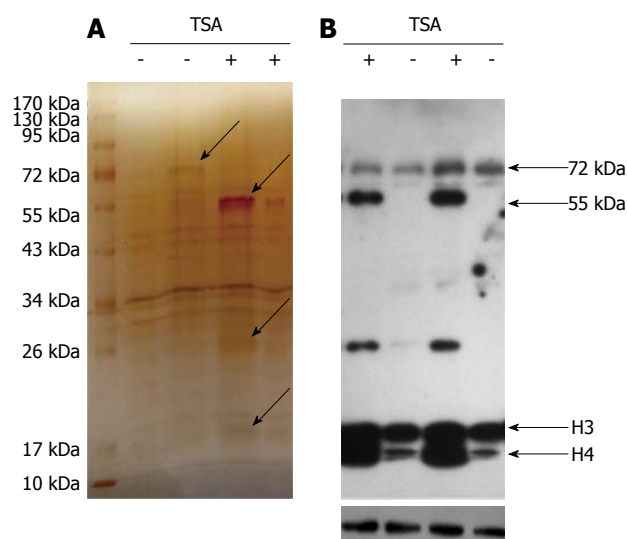


Figure 7 Identification of differential proteins of lysine acetylation after trichostatin A treatment. A: Silver staining showed the differential proteins of lysine acetylation in AGS cells after trichostatin A (TSA) treatment; B: Western blotting showed the differential proteins of lysine acetylation in AGS cells after TSA treatment, “-” before TSA intervention; “+” after TSA intervention, Acetyl- α -tubulin (Lys40) (D20G3) XP[®] Rabbit mAb was the primary antibody and Goat anti-rabbit IgG-HRP was the secondary antibody.

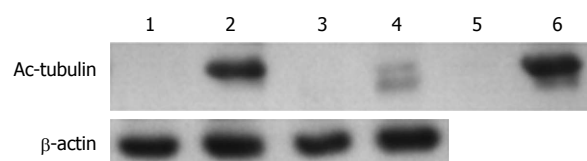


Figure 8 Identification of the effectiveness of lysine-acetylated antibodies enriching acetylated proteins. Line 1: 20 μg total protein from AGS cells unexposed to trichostatin A (TSA); Line 2: 20 μg total protein from AGS cells exposed to 0.5 $\mu\text{mol/L}$ TSA; Line 3: 20 μg flow-through protein from AGS cells unexposed to TSA, which was incubated with an antibody gel column; Line 4: 20 μg flow-through protein from AGS cells exposed to 0.5 $\mu\text{mol/L}$ TSA, which was incubated with an antibody gel column; Line 5: 100 ng enriched protein from AGS cells unexposed to TSA, which was incubated with an antibody gel column; and Line 6: 100 ng enriched protein from AGS cells exposed to 0.5 $\mu\text{mol/L}$ TSA, which was incubated with an antibody gel column.

the present study, cycle arrest in G0/G1 phase was more obvious.

Current studies indicate that TSA can activate histone acetylation to loosen the chromosome structure, thus endonuclease can easily access DNA, and TSA can block signal transduction pathways associated with cell proliferation by activating death receptors and mitochondrial apoptotic pathways, promoting transcription of tumor suppressor genes, which directly or indirectly induces tumor cell apoptosis^[23,24]. Our research showed that the expression levels of tumor suppressor genes, p21, p53 and Bax, were increased after AGS cells were exposed to 0.25 $\mu\text{mol/L}$ TSA, which increased with treatment duration, and the protooncogenes Bcl-2, CDK2 and CyclinD1 showed the opposite trend. These results are consistent with those of previous publications^[22,25-29], but different from some reports. The research of Suzuki *et al.*^[20] showed that TSA could reduce p53 expression level, although

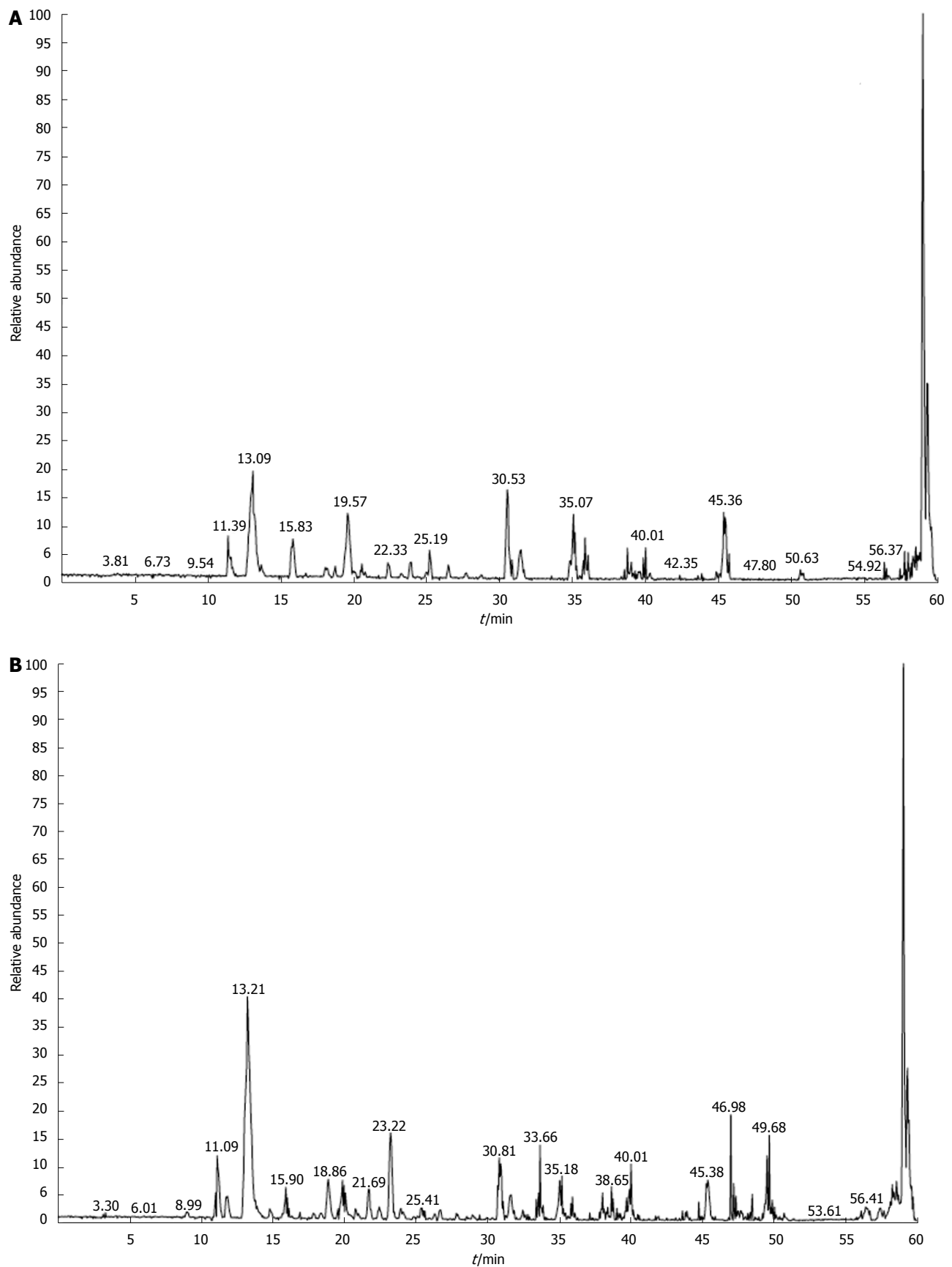


Figure 9 Mass spectrometry total ion chromatography. A: 72 kDa band of lysine-acetylated protein in AGS cells before trichostatin A (TSA) treatment; B: 28 kDa band of lysine-acetylated protein in AGS cells after TSA treatment.

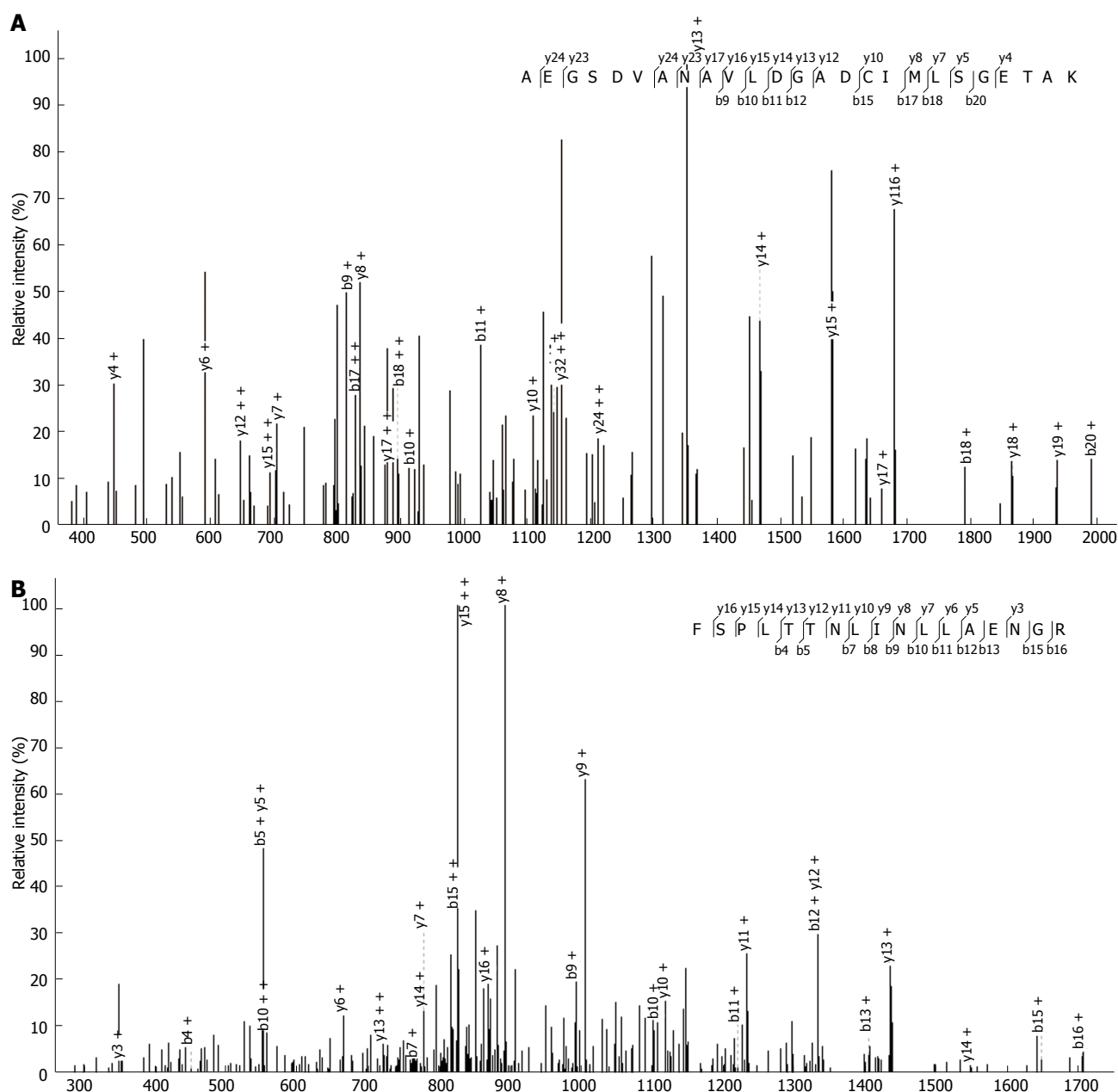


Figure 10 Mass spectrometry identification of peptides from silver staining gel. Mass spectra of 2 acetylated peptides from PKM2 and ATP5O are presented. A: PKM2 "AEGSDVANAVLDGADCIMLSGETAK"; B: ATP5O "FSPLTTNLLNLAENGR".

p21 and Bax expression levels were enhanced. The research of Juan *et al.*^[30] showed that deacetyltransferase can specifically lower *p53* and *p53*-dependent genes. These different results may be the result of different group designs and study objectives, which need to be confirmed. In most research studies, *P21waf1/cip1* is used as the transcript of target gene at *p53* downstream, a suppressor of cyclin and cyclin-dependent kinase, which can be combined with a variety of cyclins/CDK complexes by phosphorylation to inhibit cell growth in G2/M phase, thus inhibiting proliferation of tumor cells. It is believed that *P21waf1/cip1* silencing mechanisms in tumor cells may be decided by epigenetic modifications of their chromatin, and their expression levels are regulated by histone acetylation^[31]. Some research studies confirmed that HDACi-

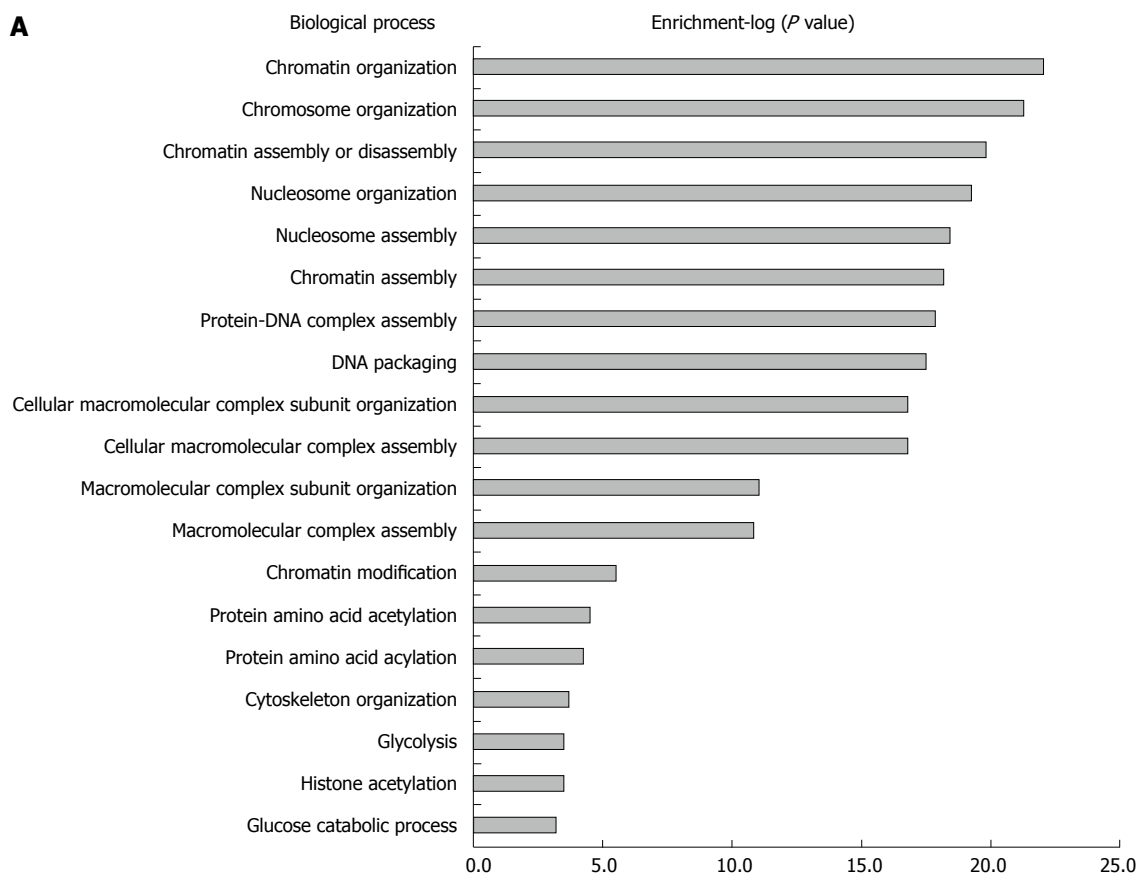
induced histone is acetylated in the *P21waf1/cip1* gene promoter region, and *P21waf1/cip1* may be a direct target of TSA^[32].

It is clear that TSA plays a role in histone acetylation, however, the function of TSA in non-histone acetylation in the inhibition of tumor growth has rarely been reported. Therefore, we immunoprecipitated AGS cells before and after exposure to TSA with lysine-acetylated monoclonal antibodies, and found an enriched protein band at 72 kDa before exposure and three enriched protein bands at 55, 28 and 17 kDa after exposure. The enriched proteins at 55 and 17 kDa were found to be tubulin and histone, respectively. We extracted two unknown protein bands at 72 and 28 kDa with gel and identified them by in-gel mass spectrometry and found that the 28 kDa

Table 2 Proteomic identification of acetylated proteins in AGS cells

Reference	Sequence
Filamin A, alpha	K.TGVAVNKPAEFTVDAK*HGGK.A
Heat shock cognate 71 kDa protein	R.RFDDAVVQSDMK*HWPFMVVNDAGRPK.H
Heat shock protein HSP 90-alpha	R.MKENQK*HIYYITGETK.D
	R.MK*ENQKHIYYITGETK.D
Histone H2B type 1-C/E/F/G/I	M.PEPAK*SAPAPK*K*GSK*K*AVTK*AQK.K
	R.LLLPGELAK*HAVSEGK.A
Histone H2B type 1-D	K.SAPAPK*K*GSK*K*AVTK*AQK*K.D
Histone H2B type 1-H	K.#KGSK*K*AVTK*AQK*K.D
Histone H2B type 2	K.SAPAPK*K*GSK*K*AVTK*VQK.K
Ezrin	R.QAVDQIK*SQEQLAAELAEYTAI.I
Histone H4	M.SGRGK*GGK*GLGK*GGAK*R.H
Fructose-bisphosphate aldolase A	K.DGADFAK*WR.C
Histone H2B type 1-B	K.K*GSK*K*AITK*AQK*K.D
	K.SAPAPK*K*GSK*K*AITK*AQK.K
	R.LLLPGELAK*HAVSEGK.A
Tubulin beta chain	R.ISVYYNEATGGK*YVPR.A
Histone H2B type 1-M	K.K*GSK*K*AINK*AQK.K
T-complex protein 1 subunit theta	K.EGAK*HFSGLEEAVYR.N
Tubulin beta-4B chain	R.INVYYNEATGGK*YVPR.A
Uncharacterized protein	K.HELQANCYEEVK*DR.C
Histone H3	R.K*QLATK*AAR.K
	R.K*STGGK*APR.K
Glyceraldehyde-3-phosphate dehydrogenase	R.VIISAPSADAPMFVMGVNHEK*YDNSLK.I
Heterogeneous nuclear ribonucleoprotein Q	K.SAFLCGVMK*TYR.Q
Phosphoglycerate kinase 1	R.FHVEEGK*GK.D
Histone H3.1t	R.EIAQDFK*TDLR.F
T-complex protein 1 subunit alpha	K.DDK*HGSYEDAVHSGALND.-
Phosphoglycerate mutase 1	K.AETAAK*HGEAQVK.I
Nucleophosmin	K.VEAK*FINYVK.N
60S ribosomal protein L3	K.FIDTTSK*FGHGR.F
ADP/ATP translocase 3	K.QIFLGGVDK*HTQFWR.Y
U1 small nuclear ribonucleoprotein 70 kDa	R.VNYDTTESK*LR.R
ATP5O ATP synthase subunit O, mitochondrial	GEVPCTVTSASPLEEATLSELK*TVLK
CREB-binding protein	K.#KK*NNK*K*TNK*NK*SSISR.A
	K.SHAHK*MVK*WGLGLDDEGSSQGEPQSK*SPQESR.R
	R.KKEESTAASETTEGSQGDGSK*NAK*K.K
HUMAN Histone H2A.Z	M.AGGK*AGK*DSGK*AK*TK.A
Uncharacterized protein	K.FK*YDDAER.R
Uncharacterized protein	K.SAFLCGVMK*TYR.Q
Heat shock protein beta-1	K.DGVVEITGK*HEER.Q
T-complex protein 1 subunit beta	R.EALLSSAVDHGSDEVK*FR.Q
Galectin-1	K.LPDGYEFK*FPNR.L
Histone H2A type 1-H	R.GK*QGGK*AR.A
Asparagine synthetase	K.VASVEMVK*YHHC.R
Retinoblastoma binding protein 7	K.IECEIK*INHEGEVNR.A
Glucose-6-phosphate isomerase	R.SGDWK*GYTGK.T
Uncharacterized protein	R.EQCCYNCGK*PGHLAR.D
Uncharacterized protein	K.IASK*YDHQAEEDLR.N
Actin-related protein 3	K.EFNK*YDTDGSK.W
Histone H2A type 2-B	R.GK*QGGK*AR.A
Uncharacterized protein	K.ITIMPK*.H
Programmed cell death protein 5	K.HGDPGDAAQQEAK*HR.E
Fumarate hydratase, mitochondrial	K.VPNDK*YYGAQTVR.S
Lamin-B receptor	K.YGVAWEK*YCQR.V
Uncharacterized protein	K.VTGLETK*YK.W
PC4 and SFRS1-interacting protein	K.TKDQGK*K*GPNK*K*.L
26S protease regulatory subunit 10B	K.VVSSIVDK*YIGESAR.L
Hematological and neurological expressed 1 protein	R.RNPPGGK*SSLVLG.-
Uncharacterized protein	R.LNQVIFPVSYNDK*FYK.D
Acyl-CoA-binding protein	K.TK*PSDEEM@LFIYGHYK.Q
Probable global transcription activator SNF2L2	K.K*GK*GGAK.T
Chromodomain-helicase-DNA-binding protein 4	R.NLGK*GK.R
Biorientation of chromosomes in cell division protein 1-like	K.SLLEEK*LVLK*SK*S
Aspartate aminotransferase	R.DVFLPK*PTWGNHTPIFR.D
Histone-lysine N-methyltransferase MLL3	K.TLVLSDK*HSPQK*K.S
Bromodomain-containing protein 1	R.HPSSPCSVK*HSPTR.E
LINE-1 type transposase domain-containing protein 1	R.KFQK*LKNKEEVK*.A

B-cell CLL/lymphoma 9-like protein	R.GHCPPAPAK*PMHPENK*LTNHGK.T
WD repeat-containing protein 46	M.ETAPK*PGK.D
Metastasis-associated protein MTA2	R.VGCK*YQAEIPDR.L
Cyclin-dependent kinase 11B	R.SHSAEGGK*HAR.V
Homeobox protein Hox-C8	R.YQTLELEK*.E
Ubiquitin carboxyl-terminal hydrolase 8	R.KEEQEQK*AKK*K.Q
28S ribosomal protein S9, mitochondrial	K.AEAIVYK*HGSGR.I
GDNF family receptor alpha-like	K.K*CINKSDNVK*EDK*FK.W
Solute carrier organic anion transporter family member 4C1	K.FGK*SIK.D
Ovochymase-1	R.#GAFGISYIDLK*VLGPK.D
Coiled-coil domain-containing protein 13	K.KKIEEDRFAFTGTAGVAGDVVATK*.I
Threonine synthase-like 1	K.LSCGEWK*SLVGATYVER.A
Secreted frizzled-related protein 1	K.K*K*DLKKLVLYLK*.N
Dynein heavy chain 3, axonemal	R.LREAEGKLAQMOK*.L
Histone acetyltransferase KAT6B	R.#QSPAKVQSK*NK*YLHSPESR.P !
Polycomb protein SCMH1	R.KPGK*K*R.G
Zinc finger protein 512B	K.#EK*K*K*NLGGK*K*.R
Dedicator of cytokinesis protein 7	R.AHGELHEQFK*R.K
Remodeling and spacing factor 1	R.GK*DISTITGHR.G
HIRA-interacting protein 3	R.#TQLKGGK*R.L
Ubiquitin-fold modifier-conjugating enzyme 1	K.ICLTDHFK*PLWAR.N
Uncharacterized protein	K.QNKTk*R.Q
Chromosome 1 open reading frame 149	R.YLTNQK*NSNSK*NDR.R
Uncharacterized protein	K.#EK*GDK*K*EGKDVK*.V
Uncharacterized protein	K.NLACEESK*R.K
Ubiquitin carboxyl-terminal hydrolase	R.DLLQFFK*PR.Q
Uncharacterized protein	R.YLVASK*.E



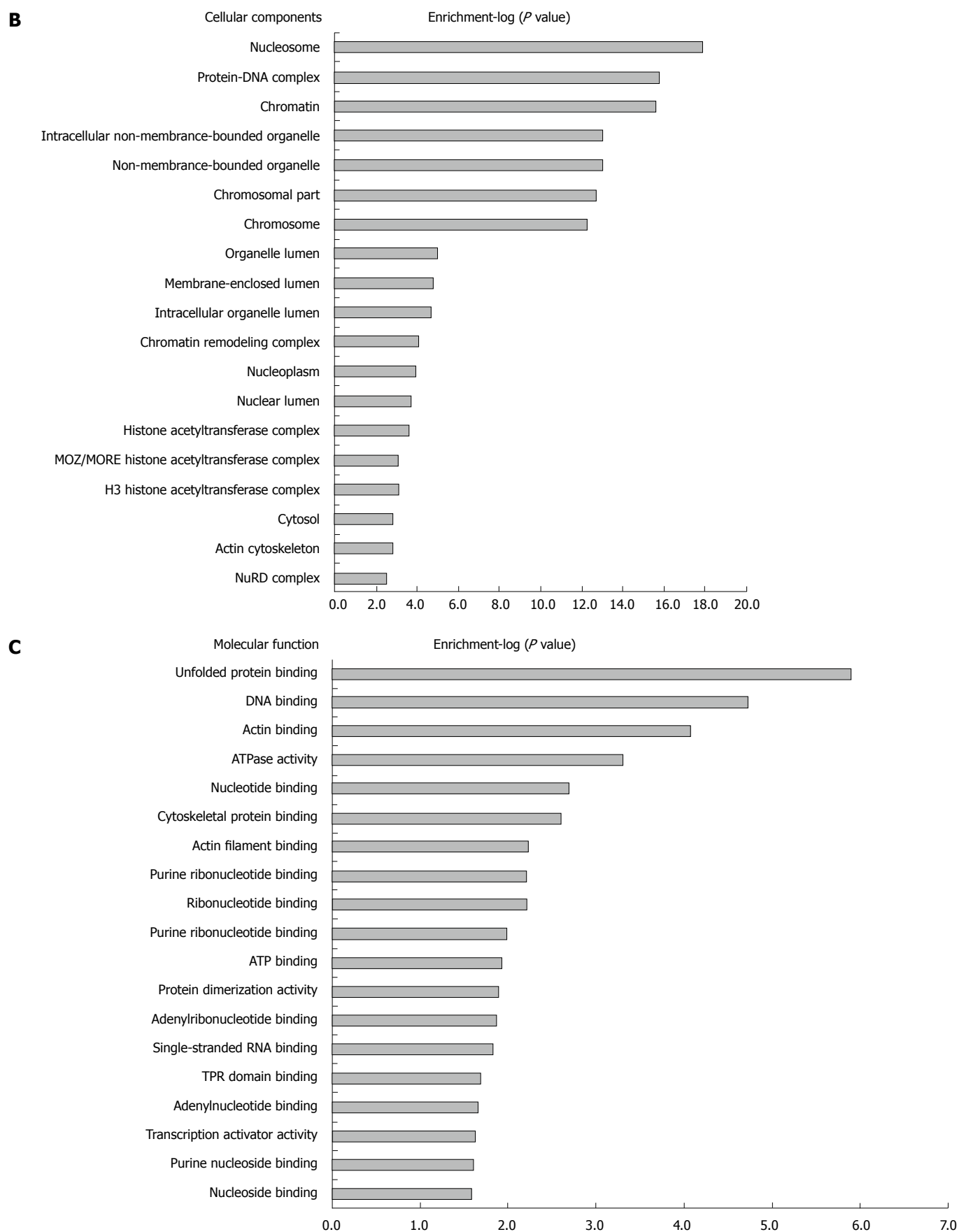


Figure 11 G0 contents based on biological process, cellular components and molecular function in which differently modified proteins were significantly enriched. A: Biological process; B: Cellular components; C: Molecular function.

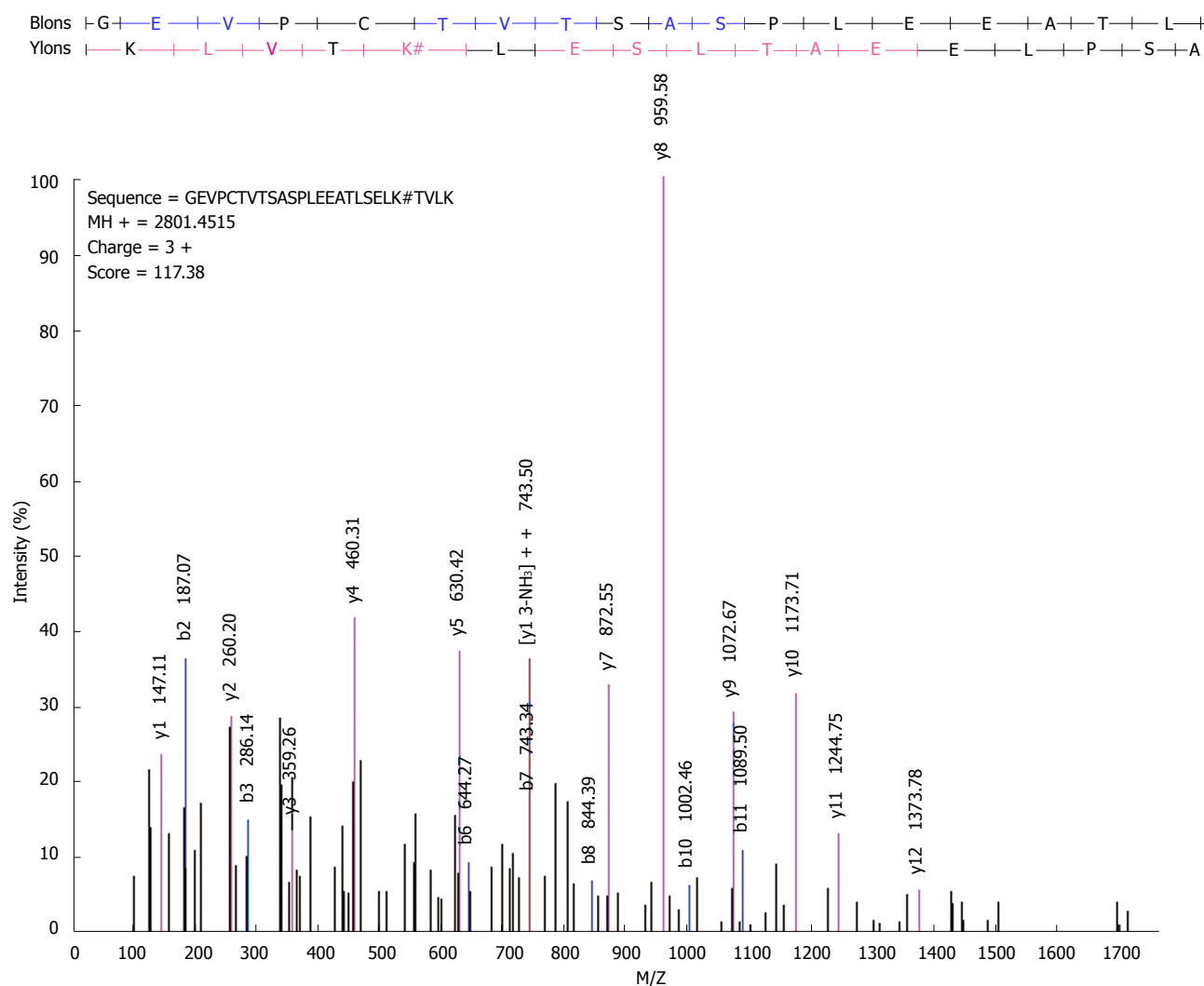


Figure 12 High-resolution MS/MS spectra of acetylated peptide at lysine 158 (GEVPCTVTSASPLEEATLSELK*TVLK) in ATP5O.

protein band was ATP5O. To further determine whether ATP5O showed lysine acetylation, we performed mass spectrometry on the acetylated sites of normal AGS cells. The results confirmed that ATP5O had acetylated sites. The verification experiment of acetylated protein showed that the degree of acetylation of ATP5O was increased with exposure time, while ATP5O expression level was not changed during the process. ATP5O is the main component of the oligomycin-sensitivity donor protein subunit, ATP synthase, and located in human chromosome 21q22.1-Q22.2^[33]. It is important for oxidation and phosphorylation. The component is not only associated with oxidative stress due to neurodegeneration, but also with human recombinant superoxide dismutase-1. Proteomics has become a main theme in life science research. Mass spectrometry has high sensitivity, high accuracy, and easy automation. Therefore, mass spectrometry-based identification methods have gradually become a standard for proteomics. We found that ATP5O was significantly acetylated after AGS cells were exposed to the deacetyltransferase inhibitor, TSA, using mass spectrometry technology, which indicated that the acetylation

of ATP5O was dynamically regulated in cells. At present, no ATP5O acetylation mechanisms have been reported in the domestic or international literature. Further studies are needed to determine what role this dynamic regulation plays in tumor cells and through which paths ATP5O affects tumor generation and growth after acetylation. In addition, mass spectrometry showed that a large amount of acetylated PKM2 (isoform of modified pyruvate kinase) existed in differential proteins before AGS cells were exposed to TSA, however, acetylated PKM2 was significantly reduced after exposure to TSA. PKM2 is an isoenzyme of pyruvate kinase, and a specific protein in embryos and differentiated cells^[34]. Mazurek^[35] revealed that PKM2 is a crucial factor in tumor metabolism, promoting cell proliferation and leading to tumors. Lv *et al*^[36] confirmed that PKM2 K305 acetylation decreases PKM2 enzyme activity and promotes its lysosomal-dependent degradation *via* chaperone-mediated autophagy (CMA). Acetylation increases the interaction between PKM2 and HSC70, a chaperone for CMA, and its association with lysosomes. Ectopic expression of an acetylation mimetic K305Q mutant accumulates glycolytic intermediates and

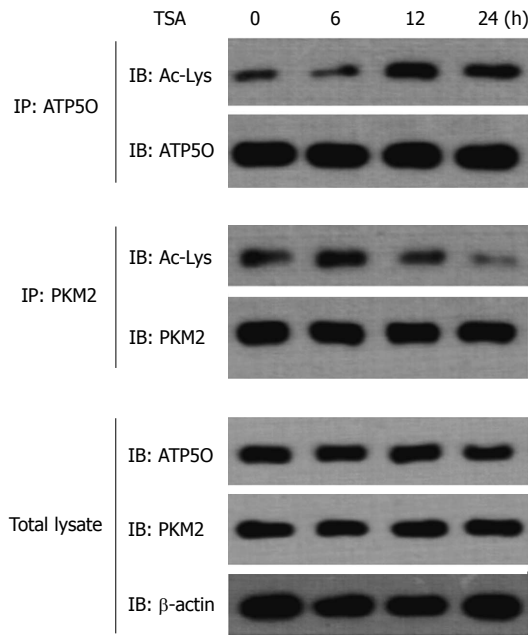


Figure 13 AGS cells were exposed to 0.5 $\mu\text{mol/L}$ trichostatin A for the indicated time periods and then ATP50 and PKM2 protein were immuno-precipitated using an anti-ATP50 antibody and an anti-PKM2 antibody. Total ATP50 and acetylation of ATP50 were detected using an anti-ATP50 antibody and an antibody specific to acetylated lysine, respectively. Total PKM2 and deacetylation of PKM2 were detected using an anti-PKM2 antibody and an antibody specific to deacetylated lysine, respectively. ATP50, PKM2 and β -Actin protein levels in the total lysate are also shown.

promotes cell proliferation and tumor growth. Further research is required on why acetylated PKM2 is reduced after AGS cells are exposed to TSA, what mechanisms affect the process, and whether TSA induces PKM2 deacetylation by activating other signaling pathways.

One field of tumor research is to explore deacetyltransferase inhibitors which have little toxicity and good efficacy, and combine deacetyltransferase inhibitors with clinical cancer treatment, including the combination of deacetyltransferase inhibitors with chemotherapeutics or with gene therapies or other tumor apoptosis or differentiation-inducing agents to determine better individual therapy for all tumors. Our experiments demonstrated that TSA played a role in inhibiting proliferation, promoting apoptosis and affecting the normal cell cycle of AGS cells. Besides activation of a variety of tumor-related signaling pathways and involvement in histone acetylation, TSA may also influence the growth and metabolism of gastric cancer cells by acetylation of non-histone, such as modification of ATP50. Exploring more deacetyltransferase inhibitors and their action sites is favorable in the development of new drugs.

COMMENTS

Background

The prevalence and mortality of gastric cancer in East Asia are higher than the world average values. In China, more than 400000 new patients are diagnosed every year. In absence of targets, the traditional chemotherapies have severe side effect. Therefore cancer treatment and research are now focusing on the

molecular targeted therapy due to its high selectivity, good efficacy and little side effects.

Research frontiers

This study is the first to select acetylated differential proteins before and after gastric cancer cells are exposed to trichostatin A (TSA) to explore the effect of lysine acetylation of related proteins on regulating the proliferation of gastric cancer cells. Moreover, sketch the lysine-acetylated proteins and the modified sites of AGS cells.

Innovations and breakthroughs

Previous researches are with the acetylation modification of deacetyltransferase inhibitor on histone, but rare studies focus on the acetylation modification of deacetyltransferase on non-histone. The study is on whether the acetylated non-histones is involved in tumor growth and metabolism, a high-resolution mass spectrometer is applied to detect the acetylated proteins and modified sites.

Applications

The study provides an experimental basis for future studies on exploring more deacetyltransferase inhibitors and action sites thereof is favorable to the development of new drugs for cancer.

Peer review

The authors explored TSA can inhibit gastric cancer cell proliferation and ATP50 was obviously acetylated after TSA intervenes. Simultaneously, they sketched the acetylated proteins and modified sites in AGS cells. The paper is well presented and the results are interesting.

REFERENCES

- Krejs GJ. Gastric cancer: epidemiology and risk factors. *Dig Dis* 2010; **28**: 600-603 [PMID: 21088409 DOI: 10.1159/000320277]
- Jemal A, Bray F, Center MM, Ferlay J, Ward E, Forman D. Global cancer statistics. *CA Cancer J Clin* 2011; **61**: 69-90 [PMID: 21296855 DOI: 10.3322/caac.20107]
- Yang L. Incidence and mortality of gastric cancer in China. *World J Gastroenterol* 2006; **12**: 17-20 [PMID: 16440411]
- Dhordain P, Lin RJ, Quief S, Lantoine D, Kerckaert JP, Evans RM, Albagli O. The LAZ3(BCL-6) oncoprotein recruits a SMRT/mSIN3A/histone deacetylase containing complex to mediate transcriptional repression. *Nucleic Acids Res* 1998; **26**: 4645-4651 [PMID: 9753732]
- Balaguer TM, Gómez-Martínez A, García-Morales P, Lacueva J, Calpena R, Reverte LR, Riquelme NL, Martínez-Lacaci I, Ferragut JA, Saceda M. Dual regulation of P-glycoprotein expression by trichostatin A in cancer cell lines. *BMC Mol Biol* 2012; **13**: 25 [PMID: 22846052 DOI: 10.1186/1471-2199-13-25]
- Zhang QC, Jiang SJ, Zhang S, Ma XB. Histone deacetylase inhibitor trichostatin A enhances anti-tumor effects of docetaxel or erlotinib in A549 cell line. *Asian Pac J Cancer Prev* 2012; **13**: 3471-3476 [PMID: 22994780]
- Su L, Xu G, Shen J, Tuo Y, Zhang X, Jia S, Chen Z, Su X. Anticancer bioactive peptide suppresses human gastric cancer growth through modulation of apoptosis and the cell cycle. *Oncol Rep* 2010; **23**: 3-9 [PMID: 19956858]
- Guan KL, Yu W, Lin Y, Xiong Y, Zhao S. Generation of acetyllysine antibodies and affinity enrichment of acetylated peptides. *Nat Protoc* 2010; **5**: 1583-1595 [PMID: 21085124 DOI: 10.1038/nprot.2010.117]
- Chen Y, Kwon SW, Kim SC, Zhao Y. Integrated approach for manual evaluation of peptides identified by searching protein sequence databases with tandem mass spectra. *J Proteome Res* 2005; **4**: 998-1005 [PMID: 15952748 DOI: 10.1021/pr049754t]
- Vadineanu A, Berden JA, Slater EC. Proteins required for the binding of mitochondrial ATPase to the mitochondrial inner membrane. *Biochim Biophys Acta* 1976; **449**: 468-479 [PMID: 136985]
- Willingham MC, Rutherford AV, Cheng SY. Immunohistochemical localization of a thyroid hormone-binding protein (p55) in human tissues. *J Histochem Cytochem* 1987; **35**: 1043-1046 [PMID: 3305699]
- Rodríguez-Paredes M, Esteller M. Cancer epigenetics reach-

- es mainstream oncology. *Nat Med* 2011; **17**: 330-339 [PMID: 21386836 DOI: 10.1038/nm.2305]
- 13 **Cortez CC**, Jones PA. Chromatin, cancer and drug therapies. *Mutat Res* 2008; **647**: 44-51 [PMID: 18691602 DOI: 10.1016/j.mrfmmm.2008.07.006]
- 14 **Ma P**, Pan H, Montgomery RL, Olson EN, Schultz RM. Compensatory functions of histone deacetylase 1 (HDAC1) and HDAC2 regulate transcription and apoptosis during mouse oocyte development. *Proc Natl Acad Sci USA* 2012; **109**: E481-E489 [PMID: 22223663 DOI: 10.1073/pnas.1118403109]
- 15 **Marks PA**, Richon VM, Breslow R, Rifkind RA. Histone deacetylase inhibitors as new cancer drugs. *Curr Opin Oncol* 2001; **13**: 477-483 [PMID: 11673688]
- 16 **Takai N**, Ueda T, Nishida M, Nasu K, Narahara H. A novel histone deacetylase inhibitor, Scriptaid, induces growth inhibition, cell cycle arrest and apoptosis in human endometrial cancer and ovarian cancer cells. *Int J Mol Med* 2006; **17**: 323-329 [PMID: 16391833]
- 17 **Chang J**, Varghese DS, Gillam MC, Peyton M, Modi B, Schiltz RL, Girard L, Martinez ED. Differential response of cancer cells to HDAC inhibitors trichostatin A and depsipeptide. *Br J Cancer* 2012; **106**: 116-125 [PMID: 22158273 DOI: 10.1038/bjc.2011.532]
- 18 **Agudelo M**, Gandhi N, Saiyed Z, Pichili V, Thangavel S, Khatavkar P, Yndart-Arias A, Nair M. Effects of alcohol on histone deacetylase 2 (HDAC2) and the neuroprotective role of trichostatin A (TSA). *Alcohol Clin Exp Res* 2011; **35**: 1550-1556 [PMID: 21447001 DOI: 10.1111/j.1530-0277.2011.01492.x]
- 19 **Meng J**, Zhang HH, Zhou CX, Li C, Zhang F, Mei QB. The histone deacetylase inhibitor trichostatin A induces cell cycle arrest and apoptosis in colorectal cancer cells via p53-dependent and -independent pathways. *Oncol Rep* 2012; **28**: 384-388 [PMID: 22552631 DOI: 10.3892/or.2012.1793]
- 20 **Suzuki T**, Yokozaki H, Kuniyasu H, Hayashi K, Naka K, Ono S, Ishikawa T, Tahara E, Yasui W. Effect of trichostatin A on cell growth and expression of cell cycle- and apoptosis-related molecules in human gastric and oral carcinoma cell lines. *Int J Cancer* 2000; **88**: 992-997 [PMID: 11093826]
- 21 **Zou XM**, Li YL, Wang H, Cui W, Li XL, Fu SB, Jiang HC. Gastric cancer cell lines induced by trichostatin A. *World J Gastroenterol* 2008; **14**: 4810-4815 [PMID: 18720545]
- 22 **Anh TD**, Ahn MY, Kim SA, Yoon JH, Ahn SG. The histone deacetylase inhibitor, Trichostatin A, induces G2/M phase arrest and apoptosis in YD-10B oral squamous carcinoma cells. *Oncol Rep* 2012; **27**: 455-460 [PMID: 21993600 DOI: 10.3892/or.2011.1496]
- 23 **Chen CS**, Weng SC, Tseng PH, Lin HP, Chen CS. Histone acetylation-independent effect of histone deacetylase inhibitors on Akt through the reshuffling of protein phosphatase 1 complexes. *J Biol Chem* 2005; **280**: 38879-38887 [PMID: 16186112]
- 24 **Bártová E**, Pacherník J, Harnicarová A, Kovarik A, Kovariková M, Hofmanová J, Skalníková M, Kozubek M, Kozubek S. Nuclear levels and patterns of histone H3 modification and HP1 proteins after inhibition of histone deacetylases. *J Cell Sci* 2005; **118**: 5035-5046 [PMID: 16254244]
- 25 **Fortson WS**, Kayarthodi S, Fujimura Y, Xu H, Matthews R, Grizzle WE, Rao VN, Bhat GK, Reddy ES. Histone deacetylase inhibitors, valproic acid and trichostatin-A induce apoptosis and affect acetylation status of p53 in ERG-positive prostate cancer cells. *Int J Oncol* 2011; **39**: 111-119 [PMID: 21519790 DOI: 10.3892/ijo.2011.1014]
- 26 **Bajbouj K**, Mawrin C, Hartig R, Schulze-Luehrmann J, Wilisch-Neumann A, Roessner A, Schneider-Stock R. P53-dependent antiproliferative and pro-apoptotic effects of trichostatin A (TSA) in glioblastoma cells. *J Neurooncol* 2012; **107**: 503-516 [PMID: 22270849 DOI: 10.1007/s11060-011-0791-2]
- 27 **Alao JP**, Stavropoulou AV, Lam EW, Coombes RC, Vignushin DM. Histone deacetylase inhibitor, trichostatin A induces ubiquitin-dependent cyclin D1 degradation in MCF-7 breast cancer cells. *Mol Cancer* 2006; **5**: 8 [PMID: 16504004]
- 28 **Kim IA**, Shin JH, Kim IH, Kim JH, Kim JS, Wu HG, Chie EK, Ha SW, Park CI, Kao GD. Histone deacetylase inhibitor-mediated radiosensitization of human cancer cells: class differences and the potential influence of p53. *Clin Cancer Res* 2006; **12**: 940-949 [PMID: 16467109]
- 29 **Chan ST**, Yang NC, Huang CS, Liao JW, Yeh SL. Quercetin enhances the antitumor activity of trichostatin A through upregulation of p53 protein expression in vitro and in vivo. *PLoS One* 2013; **8**: e54255 [PMID: 23342112]
- 30 **Juan LJ**, Shia WJ, Chen MH, Yang WM, Seto E, Lin YS, Wu CW. Histone deacetylases specifically down-regulate p53-dependent gene activation. *J Biol Chem* 2000; **275**: 20436-20443 [PMID: 10777477]
- 31 **Gui CY**, Ngo L, Xu WS, Richon VM, Marks PA. Histone deacetylase (HDAC) inhibitor activation of p21WAF1 involves changes in promoter-associated proteins, including HDAC1. *Proc Natl Acad Sci USA* 2004; **101**: 1241-1246 [PMID: 14734806]
- 32 **Marks PA**, Breslow R. Dimethyl sulfoxide to vorinostat: development of this histone deacetylase inhibitor as an anticancer drug. *Nat Biotechnol* 2007; **25**: 84-90 [PMID: 17211407]
- 33 **Rizzardini M**, Lupi M, Mangolini A, Babetto E, Ubezio P, Cantoni L. Neurodegeneration induced by complex I inhibition in a cellular model of familial amyotrophic lateral sclerosis. *Brain Res Bull* 2006; **69**: 465-474 [PMID: 16624679]
- 34 **Gupta V**, Bamezai RN. Human pyruvate kinase M2: a multifunctional protein. *Protein Sci* 2010; **19**: 2031-2044 [PMID: 20857498 DOI: 10.1002/pro.505]
- 35 **Mazurek S**. Pyruvate kinase type M2: a key regulator of the metabolic budget system in tumor cells. *Int J Biochem Cell Biol* 2011; **43**: 969-980 [PMID: 20156581 DOI: 10.1016/j.biocel.2010.02.005]
- 36 **Lv L**, Li D, Zhao D, Lin R, Chu Y, Zhang H, Zha Z, Liu Y, Li Z, Xu Y, Wang G, Huang Y, Xiong Y, Guan KL, Lei QY. Acetylation targets the M2 isoform of pyruvate kinase for degradation through chaperone-mediated autophagy and promotes tumor growth. *Mol Cell* 2011; **42**: 719-730 [PMID: 21700219 DOI: 10.1016/j.molcel.2011.04.025]

P- Reviewers Demonacos C, Mimeault M **S- Editor** Wen LL
L- Editor A **E- Editor** Li JY

